Eur. Phys. J. Plus (2023) 138:751
https://doi.org/10.1140/epjp/s13360-023-04377-4

THE EUROPEAN PHYSICAL JOURNAL PLUS

Regular Article

Monte Carlo simulations of the underwater detection of illicit war remnants with neutron-based sensors

Michał Silarski[1,a], Paweł Sibczyński[1], Oleg Bezshyyko[2], Łukasz Kapłon[1,5], Vinod Kumar[4], Szymon Niedźwiecki[1,5], Marek Nowakowski[3], Paweł Moskal[1,5], Sushil Sharma[1,5], Franciszek Sobczuk[1]

[1] Faculty of Physics, Astronomy and Applied Computer Science, Jagiellonian University, Łojasiewicza 11, 30-348 Cracow, Poland
[2] Taras Shevchenko National University of Kyiv, Volodymyrska 60, Kyiv 01033, Ukraine
[3] Military Institute of Armoured and Automotive Technology, 05-070 Sulejowek, Poland
[4] Department of Physics, University of Lucknow, Lucknow 226007, India
[5] Center for Theranostics, Jagiellonian University, 31-348 Cracow, Poland

Received: 1 July 2023 / Accepted: 12 August 2023

Abstract In recent years, the demand for accurate detection and identification of hazardous substances in an aquatic environment, especially in the Baltic Sea, has seen a significant rise, with a specific focus on unexploded ordnance (UXO) containing conventional explosives and various chemical agents, including, but not limited to, mustard gas, Clark I and II and other lethal compounds. These substances pose a significant threat to human health and the environment, and their identification is crucial for effective demining and environmental protection efforts. In this article, a novel approach for fast, remote, and non-destructive recognition of dangerous substances based on a SABAT sensor installed on an ROV is described. The performance of the proposed neutron-based sensor in an aquatic environment was verified based on a series of Monte Carlo simulations for mustard gas, Clark I and II, and TNT, as they are the most common chemical threats at the bottom of the Baltic Sea. The sensor's ability to accurately discriminate hazardous and non-hazardous materials is described in the paper in terms of the ratio of chlorine to hydrogen (Cl/H), carbon to oxygen (C/O), and nitrogen to hydrogen (N/H) activation lines integrals. The authors also discussed the future directions of work to validate SABAT (Stoichiometry Analysis By Activation Techniques) sensors in the operational environment.

1 Introduction

Detection of threats in aquatic environments is based primarily on the determination of shapes and densities of the suspected objects. The main devices used most often in practice are sonars, radars, and magnetometers [1]. Their main disadvantage lies in the ability to determine only the position and shape of the object, without giving information about the chemical composition. Therefore, the identification of any suspicious object requires additional verification or sample collection which may endanger the life and health of a qualified sapper. Nowadays, most often one uses an underwater ROV (Remotely Operated Vehicle), which may be used for visual inspection and sample collection and may carry several different sensors onboard. The additional verification and samples analysis is however relatively expensive and time-consuming. They are also ineffective in the case of some applications, for example, seabed demining or securing ports and offshore infrastructure, where the high rate of false-positive cases additionally increases costs and decreases the confidence of end users [2]. In particular, there are no cheap and fast methods for the safe demining of large areas of intense warfare, e.g. on the Baltic Sea, where tens of kilotons of munition were sunk during World War II. This sunken arsenal consists not only of munitions containing conventional explosives but also chemical agents, inter alia mustard gas, Clark I and II, and others [3]. Only part of the dump sites are well documented and monitored, many others have been constantly discovered by divers, fishermen, and the navy, especially along the military convoy routes. The unexploded ordnance (UXO) constitutes a threat to people and is a serious environmental problem due to shells corrosion and the possible uncontrollable release of chemical agents at the bottom of a sea. A similar ecological problem can be associated with shipwrecks which contain heavy fuel (mazut) and slowly contaminate the Sea. In this case, to assess the amount of fuel which is inside the wreck one needs to drill holes in the ship plating and take samples. In all of the examples the process of taking the material for further inspection on the board of a ship or in the laboratory is associated with a high risk of illicit substances release into the environment which in many cases makes it impossible to identify harmful agents and quantify their amount.

Limitations of commonly used methods and the growing need for mobile and non-invasive devices allowing for effective and rapid recognition of underwater threats lead to the constant search for novel solutions [4]. The main development paths in this area

[a] e-mail: michal.silarski@uj.edu.pl (corresponding author)

Published online: 25 August 2023

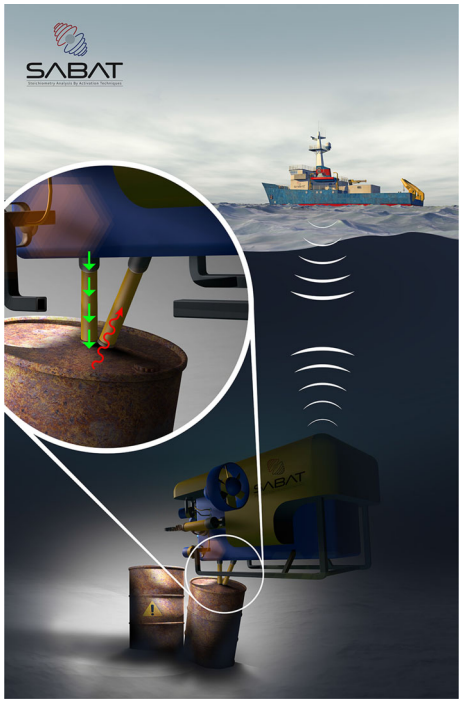

Fig. 1 Artistic view of the SABAT sensor installed on an ROV operating on the bottom of a sea and controlled by an operator on a ship. Neutrons used to excite the tested object (green arrows) are transported in a neutron guide without being attenuated in water, while the activation γ-rays (red arrow) travel in the gamma guide to the detector measuring their energy and intensity

are the existing methods with upgraded performance and usage of combinations of different sensing techniques in one detecting device [2]. There are also many trials to adopt other techniques for underwater threats detection, e.g. Raman spectroscopy [5], gravimetry [6] or Neutron Activation Analysis (NAA), which is particularly promising in terms of fast, remote and non-destructive detection and recognition of dangerous substances [7]. NAA is based on neutron capture and inelastic scattering occurring on nuclei of the investigated object which leads to their excitation. The activated nuclei deexcite to the ground state emitting γ quanta whose energies are characteristic for each isotope. These quanta can be detected by a γ spectrometer which enables reconstruction of the elemental content of the tested substance and, as a consequence, its identification [4]. The main problem limiting the sensitivity of NAA in water is a considerable background arising due to neutron interactions with the environment generating intense Oxygen and Hydrogen lines and Compton scattering continuum. Moreover, since water is one of the best moderators of neutrons the NAA sensor has to be relatively close to the tested object to obtain a significant signal-to-noise ratio. The underwater application was realized so far only within the UNCOSS project based on a sealed DT neutron source and scintillation γ quanta detector [7]. Its performance is, however, limited to the detection of objects on the bottom of the sea for which the sensor needs to approach very closely [4]. Another approach to using NAA in the aquatic environment has been developed within the SABAT project [8–13]. This sensor is based again on the usage of 14 MeV neutrons provided by a compact DT generator with Associated Particle Imagining (API) mode. API relies on the registration of the α particle originating from the DT reaction, emitted in the opposite direction to the neutron, which allows a significant suppression of detector signals which originate from the environmental background. The final design of the SABAT prototype, schematically shown in Fig. 1, assumes the usage of a compact scintillating detector made out of a $LaBr_3$:Ce,Sr scintillating crystal read out by a matrix of silicon photomultipliers (SiMPs). It will provide good energy resolution (3% at 662 keV [14]), acceptable time resolution ($\approx$700 ps [14]), and determination of the position of the gamma-ray hit with a few mm precision. Moreover, for further increase of the signal-to-noise ratio, we plan to use an active cover of the main scintillating crystal providing rejection of a vast part of the Compton-scattered γ quanta. To decrease the time needed to detect the threat, the SABAT sensor will be supplied by other devices, like e.g. magnetometer, gravimeter, or precise positioning system. The auxiliary measurements will provide fast detection of threats, even if they are hidden, and will allow estimating the distance of the sensor to the detected suspicious item. Moreover, the use of neutron and gamma quanta guides will allow to check the stoichiometry from a 10-50 cm distance [10]. Both, the background reduction and decision processes will be supported by neural network-based algorithms applied at the level of data reconstruction and analysis.

This article is a continuation of Monte Carlo simulations done for mustard gas, in which we have demonstrated that even without any background reduction techniques the detection of war remnants containing this chemical agent is feasible. It can be achieved with a sensor equipped with a $2'' \times 2''$ $LaBr_3$:Ce,Sr scintillator detector and a DT neutron generator operating in a pulsed mode with an intensity of about 10^8 neutrons per second. The best performance was achieved by separating the neutron capture $\gamma-$rays (registered after several microseconds with respect to the neutron emission) from the inelastic scattering prompt γ. The identification was performed using ratios calculated as integrals of peaks corresponding to different elements building the mustard gas: Cl/O, S/O, C/O (inelastic scattering), and Cl/H (neutron capture). Comparison of these ratios was calculated for the simulated container of

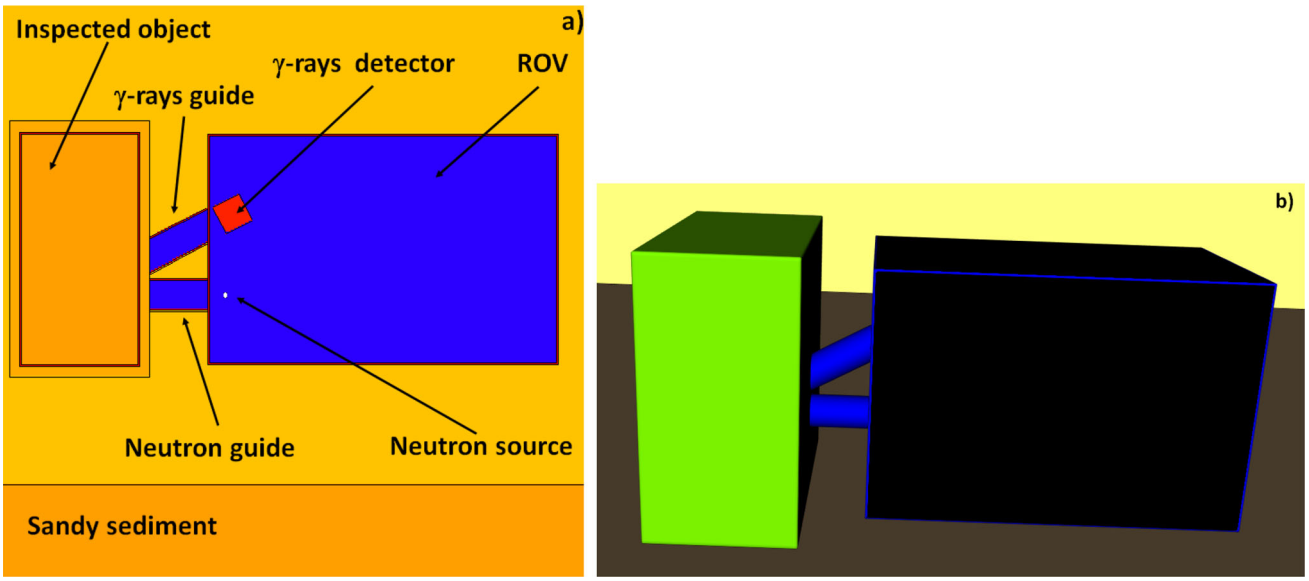

Fig. 2 **a** Side view of the Monte Carlo simulations scene. The γ quanta detector and neutron source are placed on board an ROV equipped with a neutron and γ guides. The color map corresponds to material density (blue color stands for low, yellow for medium, and red for high density); **b** a 3-D visualization of the scene used in the simulations

mustard gas ($194 \times 50 \times 50\,\mathrm{cm}^3$). These simulations showed clearly the advantage of neutron guides usage, with which the mustard gas could be effectively detected from a distance smaller than 50 cm [10]. In the next sections, we present similar simulation studies done also for the other illicit substances present on the Baltic Sea bottom: Clark I, Clark II, TNT, and heavy fuel (mazut). Here we assume the same sensor setup and a more realistic model of a ROV, on which it may be installed.

2 Materials and methods

A schematic view of the Monte Carlo simulations scene developed for our studies is shown in Fig. 2. In this exemplary figure, a $2'' \times 2''$ $LaBr_3$:Ce,Sr scintillator was set 15 cm from investigated chemical munition volume. Neutrons were generated from a point-like source placed 14 cm from the mustard gas container and at 14 cm distance from the center of the detector. The ROV was made out of 0.3 cm thick steel with dimensions $60 \times 40 \times 40\,\mathrm{cm}^3$. In order to increase the range of neutrons towards irradiated objects and decrease γ rays scattering in water volume, the ROV was equipped with cylindrical neutron and γ guides with 2" diameters and 0.3 cm thick stainless steel walls. The surrounding environment was simulated as water with 0.78% of salinity (as it is the average value for the Baltic Sea) and traces of elements taken from [15]. As a sea bottom, sandy sediment was chosen, composed of 25% of seawater and trace elements which assumed concentrations can be found in [10]. These conditions correspond to the bottom of many water reservoirs of intensive war operations close to the shores, including the Baltic Sea which is of the biggest interest. The contribution of particulated organic compounds (POC) was introduced based on data provided in [16]. We implemented this type of sediment in the simulation model, as the presence of randomly dumped chemical weapons in this region is relatively high.

Simulations were done using the MCNP v6.2 package [17] with the ENDF71x library [18] and materials composition taken from the commonly available PNNL-15870 rev. 1 library [19] implemented according to the atomic fractions. We have used the F4 flux averaged over the detector cell tally to determine the energy distribution of γ-rays reaching the detector, and the F8 pulse height tally modified with the GEB card to take into account the energy resolution of the $LaBr_3$:Ce,Sr detector, pair production, and Doppler broadening effects [4]. The energy resolution was included by a full-width-at-half-maximum (FWHM) parametrization resulting in the carbon line (4.44 MeV) resolution of about 2% [4, 10, 20]. All the spectra were generated with a 10 keV bin size and an energy threshold of 100 keV. Each of the performed simulations was done for 10^9 histories which correspond to 10 seconds of the interrogation time using the Thermo Scientific P385 pulsed D-T neutron generator providing neutron output at the level of $10^8\ \mathrm{s}^{-1}$ with a minimum pulse width of around 5 μs and fall time of 0.5 μs. The accelerator head is 686 mm in length and 102 mm in diameter [21].

As it was already mentioned, three types of chemical munition - mustard gas ($C_4H_8Cl_2S$), Clark I ($C_{12}H_{10}AsCl$) and Clark II ($C_{13}H_{10}AsN$), as well as the conventional TNT threats ($C_7H_5N_3O_6$) with different masses were modeled and analyzed. Moreover, we have made first rough checks on the possibility to detect heavy fuel (mazut) contained in many wrecks, especially in the Baltic Sea. Since densities of the studied substances contained in munition are different and changing the size could impact the resulting γ rays spectra, in the model, we assumed the same volume, amounting to 0.04 m^3, for each of the chemical agents apart from mazut,

Table 1 Most prominent γ quanta lines which may be used to identify illicit materials studied in this work

Element	Energy [MeV]	Neutron interactions process
Hydrogen	2.23	Neutron capture
Carbon	4.44	Inelastic scattering
Oxygen	6.13	Inelastic scattering
Sulfur	2.23	Inelastic scattering
Chlorine	0.79	Neutron capture
Chlorine	1.17	Neutron capture
Chlorine	1.95	Neutron capture
Chlorine	2.12	Inelastic scattering
Chlorine	6.12	Neutron capture
Chlorine	7.79	Neutron capture
Chlorine	8.58	Neutron capture
Nitrogen	10.8	Neutron capture
Nitrogen	2.31	Neutron capture
Nitrogen	5.11	Neutron capture

for which we did first preliminary studies assuming 10 times bigger volume. This is because we expect to test wrecks containing in most cases big amounts of this fuel contained in their fuel chamber.

3 Results

In order to assess the expected performance of the SABAT sensor in the detection of the substances mentioned in the previous sections, we have made the MCNP Monte Carlo simulations assuming the continuous mode of detection with no requirements on the registration time of activation γ-rays and separate detection of prompt and neutron capture radiation. As in the previous studies, we have compared the net area ratio of γ peaks identified in the simulated energy depositions spectra for elements building the studied substance. The potential lines of interest are listed in Table 1.

We have considered all the possible combinations of elemental ratios to determine the best observables for detection. Out of all the combinations we have selected the ratios between carbon and oxygen (C/O), chlorine and hydrogen (Cl/H) as well as nitrogen and hydrogen (N/H). The ratios were determined for lines with energy 2.23 MeV, 4.44 MeV, 6.12 MeV, 6.13 MeV, and 10.73 MeV for H, C, Cl, O, and N, respectively. The simulated data were processed and analyzed using MOCARZ, a dedicated open-source tool [22].The ratio uncertainties were calculated using the error propagation law using the variances of integrals for the two lines of interest. If the investigated ratio is expressed as $R = \frac{I_1}{I_2}$, and the corresponding standard deviation for the two integrated lines are σ_1 and σ_2, respectively, the uncertainty of R can be estimated using the following formula [4]:

$$\sigma_R = \sqrt{\left(\frac{\sigma_1}{I_2}\right)^2 + \left(\frac{\sigma_2 I_1}{I_2^2}\right)^2} \tag{1}$$

The simulated deposited energy distributions are presented in Fig. 3 for the continuous working mode of the neutron generator and no time gating.

In such a case neutrons are emitted in a wider time range than for prompt mode, thus, any effects of detector dead time due to high γ-rays emission rates are less probable. As expected, the environmental background, which was also simulated (Fig. 3f), is dominating the measurement and it originates mostly from the surrounding water (H and O lines and the Compton scattering continuum associated with them). Simulations show small maxima at 4.44 MeV even for background and no significant signal of the escape peaks for the carbon line (3.93 and 3.42 MeV). Such structures are quite pronounced for oxygen γ-quanta, e.g. double escape peak of 6.13 MeV line, which is, unfortunately, populating the same energy range as one of the nitrogen lines at 5.1 MeV. The same applies to γ-rays emitted by sulfur (2.23 MeV) and nitrogen (2.31 MeV) which cannot be distinguished from the hydrogen signal. The only background-free signature for nitrogen seems to be the 10.8 MeV line.

However, due to the low efficiency of the $2'' \times 2''$ LaBr3:Ce,Sr detector at this energy the expected signal for this element is very low. Taking into account simulations done before for the neutron activation sensors based on the mentioned detector and the described DT neutron generator we did not expect a very good performance of the detection, however, present studies revealed that to some extent, the continuous mode of operation can be applied to detect the relatively big amount of the studied substances if we consider the C/O elemental ratio, as shown in Table 2. Simulations show, that in the case of the Mustard Gas and Clark I, one may use also the C/H ratio, but the signal in this case is anyhow weak.

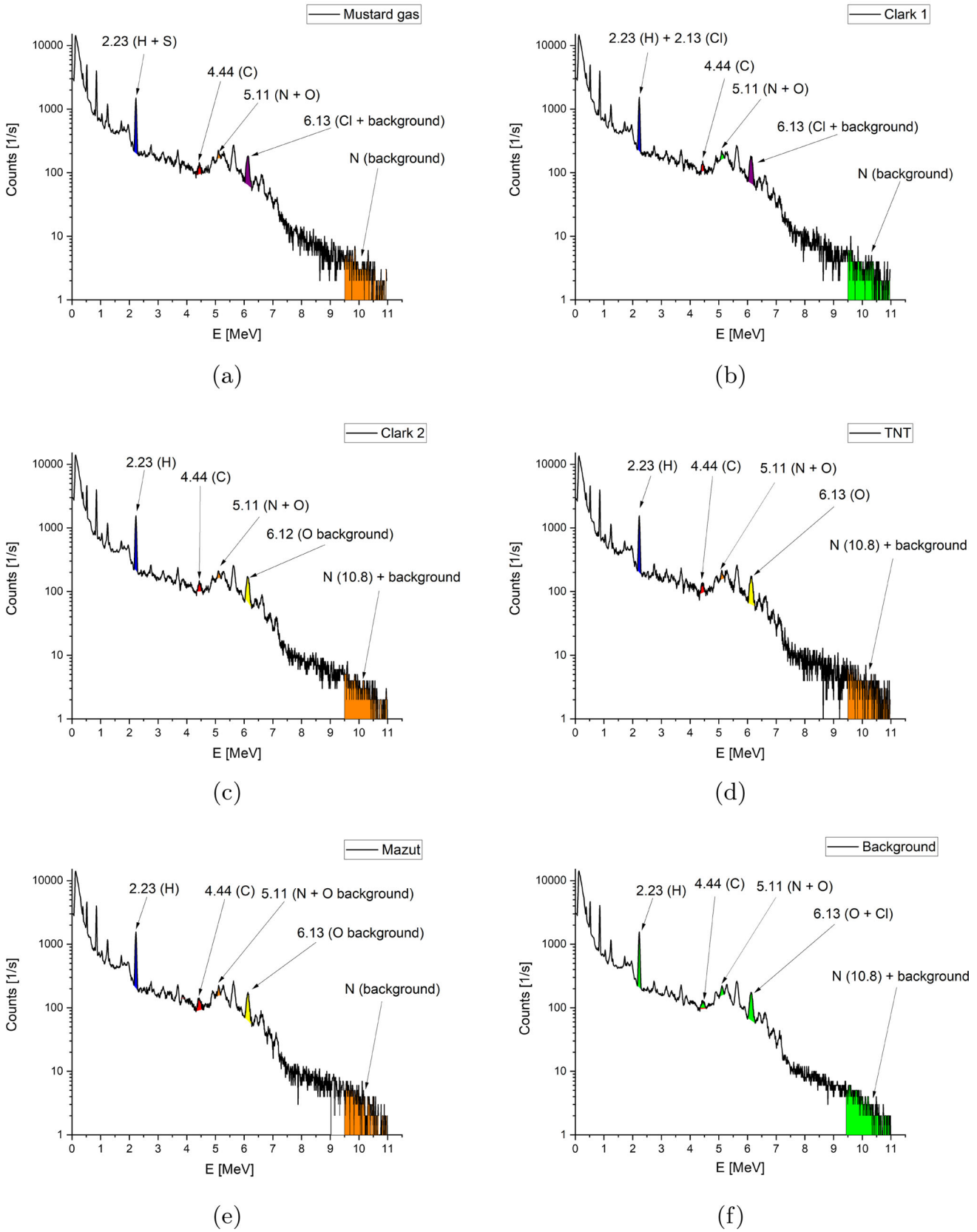

Fig. 3 γ-rays energy deposition distribution simulated for **a** Mustard gas, **b** Clark I, **c** Clark II, **d** TNT, **e** mazut, and **f** background

Table 2 Selected elemental ratios obtained from the simulations assuming continuous mode of neutron generator operation and no time gating for the sensor. The O/H ratios are close to the background value for all the materials studied showing the stability of simulation results

Chemical agent	C/O	C/H	O/H
Mustard gas	0.223 ± 0.019	0.0421 ± 0.0058	0.0879 ± 0.0085
Clark I	0.307 ± 0.025	0.0405 ± 0.0056	0.0867 ± 0.0083
Clark II	0.323 ± 0.023	0.0326 ± 0.0049	0.0750 ± 0.0076
TNT	0.274 ± 0.023	0.0349 ± 0.0050	0.0769 ± 0.0077
Mazut	0.50 ± 0.05	0.0328 ± 0.0049	0.0792 ± 0.0077
Background	0.21 ± 0.018	0.0310 ± 0.0047	0.075 ± 0.078

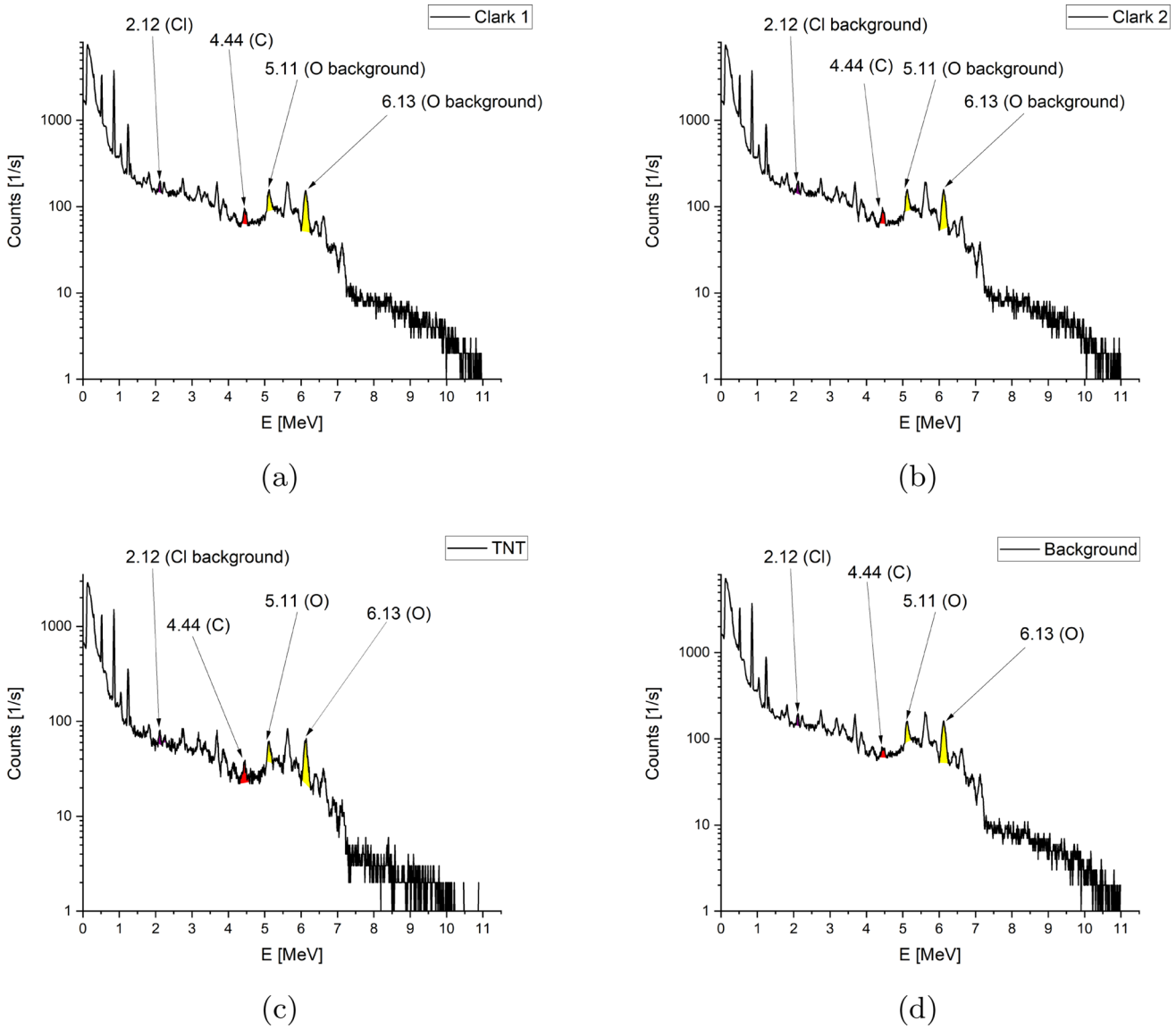

Fig. 4 γ-rays energy deposition distribution simulated for prompt gamma detection mode for **a** Clark I, **b** Clark II, **c** TNT, and **d** background

3.1 Simulations results assuming prompt gamma emission mode

In this mode, the neutron generator flux emission was set as a 2 μs pulse with flux cutoff parameter in the MCNP code implementation. The γ quanta acquisition is allowed only during that period, all neutrons after 2 μs were terminated. This time window for inelastic gamma quanta was chosen as the lowest time period (with respect to the neutron pulse generation) giving enough count rate of the prompt gammas with subsequent negligible contribution from neutron capture processes which occur later

Table 3 Carbon to oxygen elemental ratio obtained from the simulations assuming prompt gamma radiation detection

Chemical agent	C/O
Clark I	0.227 ± 0.014
Clark II	0.231 ± 0.012
TNT	0.21 ± 0.02
Background	0.122 ± 0.008

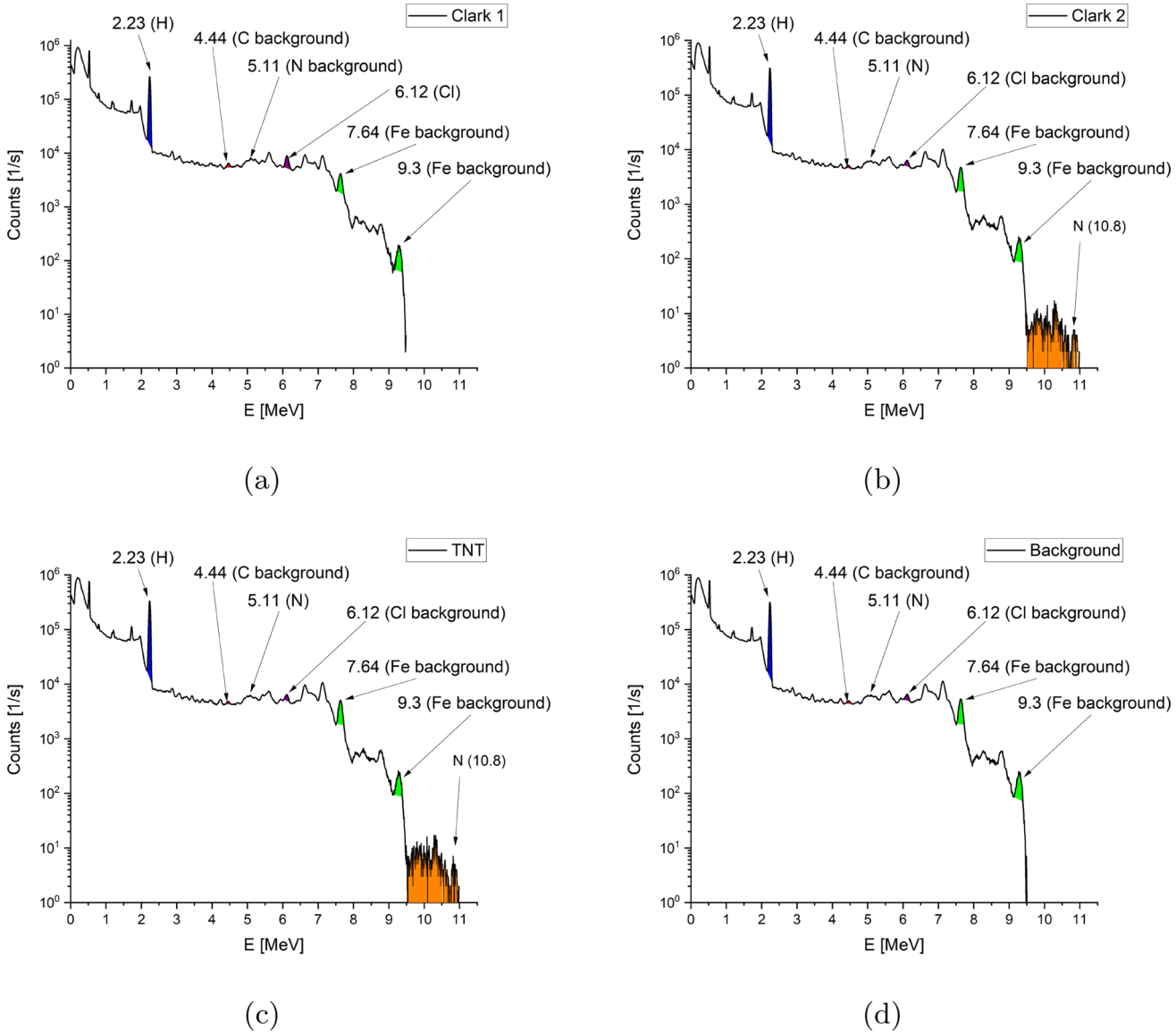

Fig. 5 γ-rays energy deposition distribution simulated for the delayed neutron capture gamma measurements for **a** Clark I, **b** Clark II, **c** TNT, and **d** background

due to the time needed to thermalize the 14 MeV neutrons. As in the case of the continuous operating mode we have analyzed the obtained energy deposition spectra shown in Fig. 4.

As one can see the hydrogen line is no more present in the obtained data indicating, that indeed the registration time cutoff at 2 μs rejects the neutron capture γ-rays.

At the same time, the oxygen line and its escape peaks are much more pronounced, as well as the other background peaks, e.g. for Si at energy 1.78 MeV or Fe at 1.27 MeV [4]. Unfortunately, this effect is not so strong in the case of the signal 4.44 MeV carbon peak. Nevertheless, we can still use the C/O ratio for the detection of Clark I, Clark II, and TNT. As we demonstrated in our previous work for the mustard gas in the prompt gamma mode detection also the Cl/O (2.12 and 6.13 MeV peaks), S/O (2.23 and

Table 4 Elemental ratios values obtained from the simulations assuming neutron capture radiation detection

Chemical agent	Cl/H	N(5.11 MeV)/H	N(10.8 MeV)/H
Clark I	0.0141 ± 0.0003	0.0026 ± 0.0001	0
Clark II	0.0044 ± 0.0002	0.0013 ± 0.0001	0.0021 ± 0.0001
TNT	0.0051 ± 0.0002	0.0017 ± 0.0001	0.0024 ± 0.0001
Background	0.0051 ± 0.0002	0.0010 ± 0.0001	0

The N(10.8 MeV)/H ratio represents all the counts integrated in the nitrogen energy range of 9.54–11 MeV and the hydrogen line. Thus, for Clark I and background, it is equal to 0 (See Fig. 5a and d)

6.13 MeV) can be used [10]. It is worth noting, that we did not perform studies separating the prompt and neutron capture γ-rays for mazut since the obtained C/O ratio for the continuous mode was significantly higher than for the background. Values of the C/O ratio for the prompt gamma mode are gathered in Table 3.

3.2 Neutron capture delayed gamma quanta mode

In the previous section, we showed the feasibility of various threats detection with two modes of neutron generator operation - with continuous and short pulse mode. Alternatively, the detection of radiation originating from neutron capture could be applied for the interrogation of objects in the aquatic environment. According to the MCNP simulations, this method is especially efficient for the detection of threats containing chlorine by comparing net peak area for Cl and H. This method could be supplementary to prompt neutron pulse and continuous neutron flux emission modes, which are useful for C/O ratio analysis. We have determined the Cl/H and N/H ratios for Clark I, Clark II, TNT, and background based on the distributions obtained in the simulations which are presented in Fig. 5. In this case, the neutron capture γ quanta for hydrogen and nitrogen are well visible, while the carbon peak is suppressed. The obtained ratios values are listed in Table 4. Our simulations show, that the separation of prompt and delayed radiation reveals a clear signal of nitrogen at the high energy manifesting itself both, in the energy distributions in Fig. 5 and in the elemental ratios.

4 Discussion

We have performed further Monte Carlo simulations of the SABAT detection system, for a more realistic geometry of the ROV, to check the performance of the detection of threats that are most commonly found on the Baltic Sea bottom in the sunken munition shells and shipwrecks: mustard gas, Clark I, Clark II, TNT and mazut. The obtained results suggest, that the successful recognition of these substances can be achieved even without the use of a neutron generator with an associated α particle system. Based on the performed MCNP simulations we conclude that both continuous mode of neutron emission, as well as pulsed one with the measurement of delayed neutron capture γ quanta detection provide sufficient performance to detect the threat. From a simulation point of view, the separate prompt γ rays emission mode would be even more efficient than the delayed radiation, especially for sulfur detection [10]. However, obtaining such a short pulse with a neutron generator would be a technical challenge. Moreover, since the neutron pulse in such an operation mode will be relatively intense another challenge arises in the design of the γ quanta detector which should be fast enough, or most likely well shielded, to prevent pile-ups and long dead times. This can be done to some extent since the currently available acquisition systems used for radiation detection offers a high sampling rate of up to 1 Mcps and often use FPGA built-in charge integration, which is suitable for high count rate measurements [23–25]. As in the previous studies, the simulations for γ-quanta originating from the neutron capture clearly show the feasibility of chlorine detection, even if it is present in the seawater. This measurement appears to be much more efficient than the detection of γ-rays with continuous neutron flux mode. For the other substances which were simulated the best observable for the detection appears to be the C/O ratio measured in the continuous neutron generator mode. Since we have simulated the same volume of each substance (apart from mazut) the results show also that the C/O ratio may be used not only to detect but also to identify the substance. This result is especially important for all the illicit substances which do not contain sulfur or chlorine which detection may support the identification (e.g. Clark II, TNT, or mazut). Unfortunately, in any simulated sensor operation mode we did not detect a significant signal for arsenic. For the nitrogen, due to the size of the γ rays detector and very low nitrogen neutron capture cross-section, the signal in the 10.8 MeV region will be measured with high uncertainty, but the simulations reveal also a possibility to detect this element via the 5.11 MeV peak. The obtained results show also, that the elemental ratios for materials that can be likely found on the bottom of the Baltic Sea are different from the ones for mustard gas (e.g. the Cl/H ratio for wood amounts to 0.014 ± 0.002) [10].

5 Conclusion

Results of the studies presented in this article constitute the next step towards building autonomous devices able to detect non-invasively hazardous materials (e.g. explosives, drugs, chemical agents) in the aquatic environment. It will contribute to increasing the safety level of civilians and critical infrastructure and to improving environmental pollution control. So far, simulations showed, that the neutron-based compact sensor with γ quanta spectrometer made of 2" × 2" $LaBr_3$:Ce,Sr crystal, and lightweight DT neutron generator will be able to identify the most common chemical agents which can be found at the bottom of the Baltic Sea within 10 s of interrogation time. The assumed amount of these substances was relatively high, but the illicit war remnants expected to be found on the bottom of the sea contain much bigger amounts of these agents. This applies especially to mazut which was an important strategic fuel used by ship fleets worldwide in the first half of the previous century. During the I and II World War, several tankers sunk on a Baltic Sea (e.g. Franken or Stuttgart), with partially filled fuel storage chambers [26]. It is commonly known that the risk of fuel unsealing becomes higher year by year leading to serious ecological disasters. The first simulation results for this substance enclosed in the 0.6 cm thick steel container showed good performance of identification of a sensor using neutron generator with associated α particle system which decreases significantly the environmental background. This conclusion should be, however, taken with care since in real conditions the performance of our sensor will strongly depend on the composition of the seabed. Thus, the next step of our work will contain an assessment of the influence of all the background-suppressing methods mentioned in Section 1. Moreover, it seems that, despite the good simulation results, much better performance may be achieved for sensors using, apart from the NAA device, also other sensors (e.g. optical) and precise positioning systems. In the case of mazut detection one of the crucial parameters, apart from the environmental background, is the thickness and structure of the wreck's hull. Thus, in the next steps, we plan to perform dedicated simulations to determine the maximum thickness of the ship side which allow for unambiguous detection of fuel. In the long-term, these simulations will open, together with detailed experimental tests in real conditions, a new path towards compact, autonomous, and fast underwater sensors based on stoichiometry determination using neutron beams, magnetometry and gravimetry, precise positioning and other auxiliary methods both underwater and on the ground. Such technology will allow for more effective and less expensive protection of the critical infrastructure against terrorism (off-shore infrastructure, airports, etc.) and safe demining of large areas of intense warfare, contributing to the solution of problems raised in the European Parliament resolution on chemical residues in the Baltic Sea [27].

Acknowledgements We acknowledge the support of Dr Neha Gupta in the editing and correcting of the manuscript.

Funding This work was supported by the EU Horizon 2020 Research and Innovation Programme under the Marie Sklodowska-Curie Grant Agreement No. 101006726, and grants U1U/P06/NW/02.07 and U1U/P07/NO/17.13 from the DigiWorld and Anthropocene Priority Research Areas under the Strategic Programme Excellence Initiative at the Jagiellonian University. We acknowledge the support from the Polish National Centre for Research and Development through Grant No. LIDER/17/ 0046/L-7/15/NCBR/2016 and from the Ministry of Education and Science through Grant No. K/PMI/000477.

Data Availability Statement This manuscript has associated data in a data repository. [Authors' comment: The datasets used and analyzed during the current study are available at: https://ujchmura-my.sharepoint.com/:f:/g/personal/michal_silarski_uj_edu_pl/EtIGtqWpuVtGoijNBWlS2b0BPc9KiMXDUFsy76s8_il3-w?e=QmmKp and from the corresponding author on reasonable request.]

References

1. T. Biobaku, G.J. Lim, J. Cho, S. Bora, H. Parsaei, Literature survey on underwater threat detection. Trans. Maritime Sci. **4**(1), 14–22 (2015). https://doi.org/10.7225/toms.v04.n01.002
2. A. Meecham, T. Acker, Underwater threat detection and tracking using multiple sensors and advanced processing, in 2016 IEEE International Carnahan Conference on Security Technology (ICCST), pp. 1–7 (2016). https://doi.org/10.1109/CCST.2016.7815723
3. A. Szarejko, J. Namieśnik, The baltic sea as a dumping site of chemical munitions and chemical warfare agents. Chem. Ecol. **25**(1), 13–26 (2009). https://doi.org/10.1080/02757540802657177
4. M. Silarski, M. Nowakowski, Performance of the sabat neutron-based explosives detector integrated with an unmanned ground vehicle: a simulation study. Sensors (2022). https://doi.org/10.3390/s22249996
5. S.K. Sharma, B.M. Howe, A.K. Misra, M.R. Rognstad, J.N. Porter, T.E. Acosta-Maeda, M.J. Egan, Underwater time-gated standoff raman sensor for in situ chemical sensing. Appl. Spectrosc. **75**(6), 739–746 (2021). https://doi.org/10.1177/00037028211001923
6. R. Mlcak, D. Doppalapudi, P. Pyzowski, P. Gwynne, S. Purchase, J. Bridgham, G. Schultz, M. Skelton, D. Pelletier, H. Tuller, Mems-based gravimetric sensors for explosives detection, in 2010 IEEE International Conference on Technologies for Homeland Security (HST), 321–324 (2010). https://doi.org/10.1109/THS.2010.5655033
7. V. Valković, 14 MeV Neutrons Physics and Application. CRC Press, Boca Raton FL 33487711, USA (2016)
8. M. Silarski, D. Hunik, P. Moskal, M. Smolis, S. Tadeja, Project of the Underwater System for Chemical Threat Detection. Acta Phys. Pol. A 127(5), 1543–1548 (2015). https://doi.org/10.12693/APhysPolA.127.1543

9. M. Silarski, Application of Neutron Activation Spectroscopy. Acta Phys. Pol. B Proc. Suppl. **6**(4), 1061–1066 (2013). https://doi.org/10.5506/APhysPolBSupp.6.1061
10. P. Sibczyński, M. Silarski, O. Bezshyyko, V. Ivanyan, E. Kubicz, S. Niedźwiecki, P. Moskal, J. Raj, S. Sharma, O. Trofimiuk, Monte carlo n-particle simulations of an underwater chemical threats detection system using neutron activation analysis. J. Instrum. **14**(09), 09001 (2019). https://doi.org/10.1088/1748-0221/14/09/P09001
11. M. Silarski, Hazardous substance detection in water environments using neutron beams : the SABAT project. Prob. Mechatron. Armament Aviat. Saf. Engi. **10**(3), 49–60 (2019). https://doi.org/10.5604/01.3001.0013.4804
12. M. Silarski, D. Hunik, M. Smolis, S. Tadeja, P. Moskal, Design of the SABAT system for underwater detection of dangerous substances. Acta Phys. Pol. B **47**(2), 497–502 (2016). https://doi.org/10.5506/APhysPolB.47.497
13. M. Silarski, P. Sibczyński, S. Niedźwiecki, S. Sharma, J. Raj, P. Moskal, Underwater detection of dangerous substances: Status of the SABAT project. Acta Physica Polonica B **48**(10) (2017). https://doi.org/10.5506/APhysPolB.48.1675
14. A. Miś, Characterization of Gamma Quanta Detector for the SABAT Sensor. Master thesis, Jagiellonian University, Kraków (2020)
15. D.A. Kulik, J. Jan Harff, Reference ion-association models of normative seawater and of Baltic sea brackish waters at salinities 1–40 permil, 1 bar total pressure and 0 to 30^0C temperature (system Na-Mg-Ca-K-Sr-Li-Rb-Cl-S-C-Br-F-B-N-Si-P-H-O. Tech. Rep. (1993). https://doi.org/10.12754/msr-1993-0006
16. T. Leipe, F. Tauber, H. Vallius, J. Virtasalo, U. Szymon, N. Kowalski, S. Hille, S. Lindgren, Particulate organic carbon (POC) in surface sediments of the Baltic Sea. Geo-Mar. Lett. **31**, 175–188 (2011). https://doi.org/10.1007/s00367-010-0223-x
17. T. Goorley, M. James, T. Booth, F. Brown, J. Bull, L.J. Cox, J. Durkee, J. Elson, M. Fensin, R.A. Forster, J. Hendricks, H.G. Hughes, R. Johns, B. Kiedrowski, R. Martz, S. Mashnik, G. McKinney, D. Pelowitz, R. Prael, J. Sweezy, L. Waters, T. Wilcox, T. Zukaitis, Initial mcnp6 release overview. Nucl. Technol. **180**(3), 298–315 (2012). https://doi.org/10.13182/NT11-135
18. J.L. Conlin, D.K. Parsons, S.J. Gardiner, A.C. Kahler III, M.B. Lee, M.C. White, M.G. Gray, Continuous energy neutron cross section data tables based upon endf/b-vii.1. Tech. Rep. (2013). https://doi.org/10.2172/1063914
19. R.J. McConn Jr, C.J. Gesh, R.T. Pagh, R.A. Rucker, R.G. Williams, Compendium of material composition data for radiation transport modeling. Tech. Rep. (2011). https://www.pnnl.gov/main/publications/external/technical_reports/PNNL-15870Rev1.pdf
20. P. Sibczynski, A. Gojska, V. Kiptily, S. Korolczuk, R. Kwiatkowski, S. Mianowski, L. Swiderski, A. Szydlowski, Characterization of some modern scintillators recommended for use on large fusion facilities in γ-ray spectroscopy and tomographic measurements of γ-emission profiles **62**, 223–228 (2017). https://doi.org/10.1515/nuka-2017-0032
21. B.A. Ludewigt, Neutron Generators for Spent Fuel Assay, LBNL-4426E, (2010)
22. P. Sibczyński, MOCARZ tool for MCNP file processing and peak fitting. https://github.com/PawelSibczynski/MOCARZ
23. S. Korolczuk, S. Mianowski, J. Rzadkiewicz, P. Sibczynski, L. Swiderski, I. Zychor, Digital acquisition in high count rate gamma-ray spectrometry. IEEE Trans. Nucl. Sci. **63**(3), 1668–1673 (2016). https://doi.org/10.1109/TNS.2016.2567455
24. G. Korcyl, P. Białas, C. Curceanu, E. Czerwiński, K. Dulski, B. Flak, A. Gajos, B. Głowacz, M. Gorgol, B.C. Hiesmayr, B. Jasińska, K. Kacprzak, M. Kajetanowicz, D. Kisielewska, P. Kowalski, T. Kozik, N. Krawczyk, W. Krzemień, E. Kubicz, M. Mohammed, S. Niedźwiecki, M. Pawlik-Niedźwiecka, M. Pałka, L. Raczyński, P. Rajda, Z. Rudy, P. Salabura, N.G. Sharma, S. Sharma, R.Y. Shopa, M. Skurzok, M. Silarski, P. Strzempek, A. Wieczorek, W. Wiślicki, R. Zaleski, B. Zgardzińska, M. Zieliński, P. Moskal, Evaluation of single-chip, real-time tomographic data processing on FPGA soc devices. IEEE Trans. Med. Imaging **37**(11), 2526–2535 (2018). https://doi.org/10.1109/TMI.2018.2837741
25. M. Silarski, K. Dziedzic-Kocurek, M. Szczepanek, Combined BNCT and PET for theranostics. Bio-Algorithms Med-Syst. **17**(4), 293–300 (2021). https://doi.org/10.1515/bams-2021-0140
26. P. Vanninen, A. Östin, J. Bełdowski, E.A. Pedersen, M. Söderström, M. Szubska, M. Grabowski, G. Siedlewicz, M. Czub, S. Popiel, J. Nawała, D. Dziedzic, J. Jakacki, B. Pączek Exposure status of sea-dumped chemical warfare agents in the baltic sea. Marine Environ. Res. **161**, 105112 (2020). https://doi.org/10.1016/j.marenvres.2020.105112
27. European Parliament resolution on chemical residues in the Baltic Sea, based on Petitions Nos 1328/2019 and 0406/2020, 2021/2567 (RSP)